# NOAA Technical Report NESS 68

U.S. DEPARTMENT OF COMMERCE
National Oceanic and Atmospheric Administration
National Environmental Satellite Service

# Dependence of Antenna Temperature on the Polarization of Emitted Radiation for a Scanning Microwave Radiometer

NORMAN C. GRODY

WASHINGTON, D.C.
January 1974

NOAA TECHNICAL REPORTS

National Environmental Satellite Service Series

The National Environmental Satellite Service (NESS) is responsible for the establishment and operation of the National Operational Meteorological Satellite System and of the environmental satellite systems of NOAA. The three principal offices of NESS are Operations, Systems Engineering, and Research. The NOAA Technical Report NESS series is used by these offices to facilitate early distribution of research results, data handling procedures, systems analyses, and other information of interest to NOAA organizations.

Publication of a report in NOAA Technical Report NESS series will not preclude later publication in an expanded or modified form in scientific journals. NESS series of NOAA Technical Reports is a continuation of, and retains the consecutive numbering sequence of, the former series, ESSA Technical Report National Environmental Satellite Center (NESC), and of the earlier series, Weather Bureau Meteorological Satellite Laboratory (MSL) Report. Reports 1 through 37 are listed in publication NESC 56 of this series.

Reports 1 through 50 in the series are available from the National Technical Information Service (NTIS), U.S. Department of Commerce, Sills Bldg., 5285 Port Royal Road, Springfield, Va. 22151. Price $3.00 paper copy; $1.45 microfiche. Order by accession number, when given, in parentheses. Beginning with 51, printed copies of the reports are available through the Superintendent of Documents, U.S. Government Printing Office, Washington, D.C. 20402. Price as indicated. Microfiche available from NTIS (use accession number when available). Price $1.45.

ESSA Technical Reports

NESC 38 Angular Distribution of Solar Radiation Reflected From Clouds as Determined From TIROS IV Radiometer Measurements. I. Ruff, R. Koffler, S. Fritz, J. S. Winston, and P. K. Rao, March 1967. (PB-174-729)

NESC 39 Motions in the Upper Troposphere as Revealed by Satellite Observed Cirrus Formations. H. McClure Johnson, October 1966. (PB-173-996)

NESC 40 Cloud Measurements Using Aircraft Time-Lapse Photography. Linwood F. Whitney, Jr., and E. Paul McClain, April 1967. (PB-174-728)

NESC 41 The SINAP Problem: Present Status and Future Prospects; Proceedings of a Conference Held at the National Environmental Satellite Center, Suitland, Maryland, January 18-20, 1967. E. Paul McClain, October 1967. (PB-176-570)

NESC 42 Operational Processing of Low Resolution Infrared (LRIR) Data From ESSA Satellites. Louis Rubin, February 1968. (PB-178-123)

NESC 43 Atlas of World Maps of Long-Wave Radiation and Albedo--for Seasons and Months Based on Measurements From TIROS IV and TIROS VII. J. S. Winston and V. Ray Taylor, September 1967. (PB-176-569)

NESC 44 Processing and Display Experiments Using Digitized ATS-1 Spin Scan Camera Data. M. B. Whitney, R. C. Doolittle, and B. Goddard, April 1968. (PB-178-424)

NESC 45 The Nature of Intermediate-Scale Cloud Spirals. Linwood F. Whitney, Jr., and Leroy D. Herman, May 1968. (AD-673-681)

NESC 46 Monthly and Seasonal Mean Global Charts of Brightness From ESSA 3 and ESSA 5 Digitized Pictures, February 1967-February 1968. V. Ray Taylor and Jay S. Winston, November 1968. (PB-180-717)

NESC 47 A Polynomial Representation of Carbon Dioxide and Water Vapor Transmission. William L. Smith, February 1969. (PB-183-296)

NESC 48 Statistical Estimation of the Atmosphere's Geopotential Height Distribution From Satellite Radiation Measurements. William L. Smith, February 1969. (PB-183-297)

NESC 49 Synoptic/Dynamic Diagnosis of a Developing Low-Level Cyclone and Its Satellite-Viewed Cloud Patterns. Harold J. Brodrick and E. Paul McClain, May 1969. (PB-184-612)

NESC 50 Estimating Maximum Wind Speed of Tropical Storms From High Resolution Infrared Data. L. F. Hubert, A. Timchalk, and S. Fritz, May 1969. (PB-184-611)

(Continued on inside back cover)

U.S. DEPARTMENT OF COMMERCE
Frederick B. Dent, Secretary

NATIONAL OCEANIC AND ATMOSPHERIC ADMINISTRATION
Robert M. White, Administrator

NATIONAL ENVIRONMENTAL SATELLITE SERVICE
David S. Johnson, Director

NOAA Technical Report NESS 68

# Dependence of Antenna Temperature on the Polarization of Emitted Radiation for a Scanning Microwave Radiometer

Norman C. Grody



WASHINGTON, D.C.
January 1974

For sale by the Superintendent of Documents, U.S. Government Printing Office, Washington, D.C. 20402. Price $0.50

CONTENTS

# DEPENDENCE OF ANTENNA TEMPERATURE ON THE POLARIZATION OF EMITTED RADIATION FOR A SCANNING MICROWAVE RADIOMETER

Norman C. Grody
National Environmental Satellite Service, NOAA, Washington, D.C.

ABSTRACT. The antenna temperature is determined for a scanning Earth-viewing satellite-borne microwave radiometer. The result is in the form of an integral that includes the antenna gain function and brightness temperature. A composite emissivity term appears in the brightness temperature equation that contains the horizontal and vertical components of surface emissivity weighted by their respective antenna gains. Analysis is performed to obtain the antenna temperature components corresponding to the emission of horizontally and vertically polarized radiation. Calculations are performed showing the effects of beam width and scan angle on the two components of antenna temperature for a linearly polarized antenna scanned about its polarization axes. Effects resulting from antenna cross-polarization are also analyzed.

## INTRODUCTION

Interpretation of radiometric data generally requires the determination of brightness temperatures from antenna temperature measurements as the first step in the complete analysis of the data. A review of some of the recent inversion techniques for estimating brightness temperatures is contained in the report by Claassen and Fung (1973). The purpose of our report, however, is to illustrate the influence of antenna characteristics, as defined by their beam width and cross polarization, on the interpretation of antenna temperature measurements for a scanning microwave radiometer. By considering simple antenna models, a number of general results are obtained that are of importance in antenna design considerations for radiometric applications.

## THEORY

Figure 1 shows the antenna coordinate system $(x',y',z')$ that is rotated by the scan angle $\phi_s$ with respect to the Earth$(x,y,z)$. Also shown is an arbitrary antenna propagation direction, as defined by the unit vector $\kappa'$, that intersects the Earth's surface where the unit normal vector is designated by $n$. In the antenna far field, the electric field received can be decomposed into the spherical components $E_{\theta'}$ and $E_{\phi'}$ as indicated in figure 1. However, with respect to the Earth coordinates, the electric field is designated by its horizontal and vertical polarization components $E_h$ and $E_v$, respectively. The total electric field $E$ can be written as

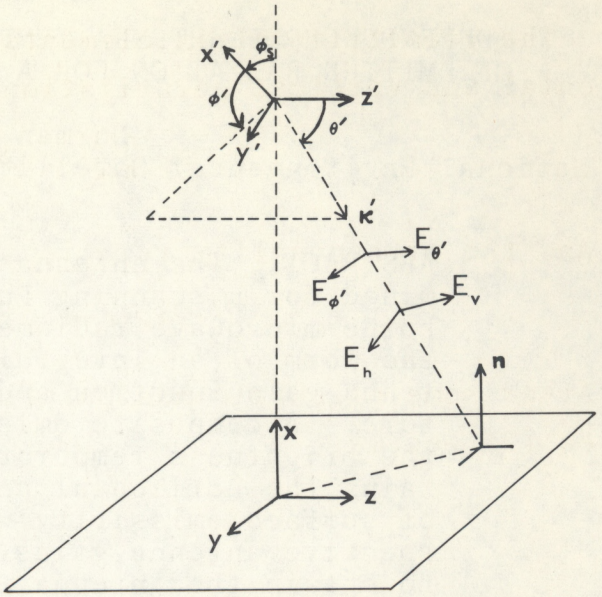


Figure 1.--Antenna and Earth coordinate systems

$$E = a_h E_h + a_v E_v = a_{\theta'} E_{\theta'} + a_{\phi'} E_{\phi'} \tag{1}$$

where the terms $a_h$, $a_v$, $a_{\theta'}$, and $a_{\phi'}$ are unit vectors that define the polarization directions of the field components.

Solving eq (1) for the antenna fields in terms of the horizontal and vertical polarization components, we find

$$\begin{pmatrix} E_{\theta'} \\ E_{\phi'} \end{pmatrix} = \begin{pmatrix} g_{11} & g_{12} \\ g_{21} & g_{22} \end{pmatrix} \begin{pmatrix} E_h \\ E_v \end{pmatrix} \tag{2}$$

where

$$g_{11} = a_{\theta'} \cdot a_h, \quad g_{12} = a_{\theta'} \cdot a_v, \quad g_{21} = a_{\phi'} \cdot a_h, \quad \text{and} \quad g_{22} = a_{\phi'} \cdot a_v .$$

The geometric matrix elements $g_{ij}$ are computed using the horizontal and vertical polarization vectors

$$a_h = \frac{n \times k'}{|n \times k'|} \quad \text{and} \quad a_v = \frac{(n \times k') \times k'}{|(n \times k') \times k'|} \tag{3}$$

and the orthogonality relationships

$$a_{\phi'} \times k' = a_{\theta'} \quad \text{and} \quad a_{\theta'} \times k' = -a_{\phi'}.$$

After some algebraic manipulations (see appendix), we find that eq (2) becomes

$$\begin{pmatrix} E_{\theta'} \\ E_{\phi'} \end{pmatrix} = \begin{pmatrix} g_{11} & \sqrt{1-g_{11}^2} \\ \sqrt{1-g_{11}^2} & -g_{11} \end{pmatrix} \begin{pmatrix} E_h \\ E_v \end{pmatrix} \tag{4a}$$

where

$$g_{11} = \frac{a_{\theta'} \cdot n}{\sqrt{1-(k' \cdot n)^2}}. \tag{4b}$$

The geometric factor $g_{11}$ is evaluated for a flat surface with its normal in the $x$ direction (fig. 1) so that

$$n = a_x = a_{x'} \cos \phi_s - a_{y'} \sin \phi_s, \tag{5a}$$

$$a_{\phi'} = -a_{x'} \sin \phi' + a_{y'} \cos \phi', \tag{5b}$$

and

$$k' = a_{x'} \sin \theta' \cos \phi' + a_{y'} \sin \theta' \sin \phi' + a_{z'} \cos \theta'. \tag{5c}$$

Substituting eq (5) into eq (4b), we find

$$g_{11} = \frac{-\sin(\phi' + \phi_s)}{\sqrt{1-\sin^2 \theta' \cos^2(\phi' + \phi_s)}} \tag{6}$$

where $g_{11}$ is a function of the scan angle $\phi_s$ and the angular coordinates $\theta'$ and $\phi'$ within the antenna beam.

The power received by an antenna $P(\phi_s)$ can be expressed in terms of the antenna gain function and far fields, namely:

$$P(\phi_s) = \left(\frac{\epsilon}{\mu}\right)^{1/2} \frac{\iint \left[G_{\theta'} |E_{\theta'}|^2 + G_{\phi'} |E_{\phi'}|^2\right] \sin \theta' \, d\theta' \, d\phi'}{\iint \left[G_{\theta'} + G_{\phi'}\right] \sin \theta' \, d\theta' \, d\phi'} \tag{7}$$

where $G_{\theta'}$ and $G_{\phi'}$ are the antenna gain functions corresponding to the $E_{\theta'}$ and $E_{\phi'}$ polarized fields, respectively. The quantities $\epsilon$ and $\mu$ respectively are the dielectric constant and permeability of the propagating media.

Substituting in eq (7) the horizontal and vertical polarization fields given by eq (4a) and ensemble averaging, we find

$$\langle P(\phi_s)\rangle = \left(\frac{\epsilon}{\mu}\right)^{1/2} \frac{\iint \left[G_h \langle |E_h|^2\rangle + G_v \langle |E_v|^2\rangle\right] \sin\theta' d\theta' d\phi'}{\iint \left[G_h + G_v\right] \sin\theta' d\theta' d\phi'}, \tag{8a}$$

$$G_h = g_{11}^2 G_{\theta'} + (1 - g_{11}^2) G_{\phi'}, \tag{8b}$$

and

$$G_v = g_{11}^2 G_{\phi'} + (1 - g_{11}^2) G_{\theta'}. \tag{8c}$$

Here, use was made of the fact that the fields $E_h$ and $E_v$ are uncorrelated random variables with zero mean so that terms involving $|E_h E_v|$ have zero average value [eq (19), Stogryn 1970].

Equation (8a) can also be written in terms of equivalent noise temperatures, namely:

$$T_a(\phi_s) = \frac{\iint \left[G_h T_h + G_v T_v\right] \sin\theta' d\theta' d\phi'}{\iint \left[G_h + G_v\right] \sin\theta' d\theta' d\phi'} \tag{9a}$$

and

$$\left(\frac{\epsilon}{\mu}\right)^{1/2} \langle |E_h|^2\rangle = \frac{4\pi}{\lambda^2} K T_h \beta \tag{9b}$$

where

$$\left(\frac{\epsilon}{\mu}\right)^{1/2} \langle |E_v|^2\rangle = \frac{4\pi}{\lambda^2} K T_v \beta \tag{9c}$$

and

$$\langle P(\phi_s)\rangle = \frac{4\pi}{\lambda^2} K T_a \beta. \tag{9d}$$

The temperatures $T_h$ and $T_v$ are the horizontal and vertical brightness temperatures; and $T_a$ is the antenna temperature, $K$ is Boltzman's constant, $\beta$ is the equivalent noise band width, and $\lambda$ is the radiation wavelength.

For a nonscattering atmosphere in local thermodynamic equilibrium, the brightness temperatures are given by

$$T_h = T_u + \tau \left[\epsilon_h T_s + (1-\epsilon_h) T_d\right] \tag{10a}$$

and

$$T_v = T_u + \tau \left[\epsilon_v T_s + (1-\epsilon_v) T_d\right] \tag{10b}$$

where $\epsilon_h$ and $\epsilon_v$ are the horizontal and vertical polarization surface emissivities and $T_s$ is the surface temperature. The temperatures $T_u$ and $T_d$ are the brightness temperature components corresponding to upward atmospheric emission from the surface to the antenna position $T_u$ and downward atmospheric radiation to the surface $T_d$. The term $\tau$ is the total atmospheric transmittance from the surface to the antenna level.

Substituting eq (10) into eq (9a), we obtain

$$T_a(\phi_s) = \frac{\iint G T_B \sin\theta' d\theta' d\phi'}{\iint G \sin\theta' d\theta' d\phi'} \tag{11a}$$

where

$$G = G_h + G_v, \tag{11b}$$

$$T_B = T_u + \tau \left[\epsilon_s T_s + (1-\epsilon_s) T_d\right], \tag{11c}$$

and

$$\epsilon_s = \frac{\epsilon_h G_h + \epsilon_v G_v}{G_h + G_v}. \tag{11d}$$

Hence, the antenna temperature is given by an integral containing the antenna gain function $G$ and a brightness temperature $T_B$. The brightness temperature equation contains a composite surface emissivity $\epsilon_s$ that depends on the horizontal and vertical emissivity components weighted by their respective antenna gains.

## LINEAR POLARIZATION RESULTS

For a linearly polarized antenna lying in the $y'$- $z'$ plane (fig. 1) with current excitation along $z'$, the far field is in the $a_{\theta'}$ direction so that $G=G_{\theta'}$. The composite emissivity then becomes

$$\epsilon_s = g_{11}^2 \epsilon_h + (1-g_{11}^2)\epsilon_v \qquad (12)$$

where the $g_{11}$ dependence of angles $\theta'$, $\phi'$, and $\phi_s$ is given by eq (6) for a flat surface.

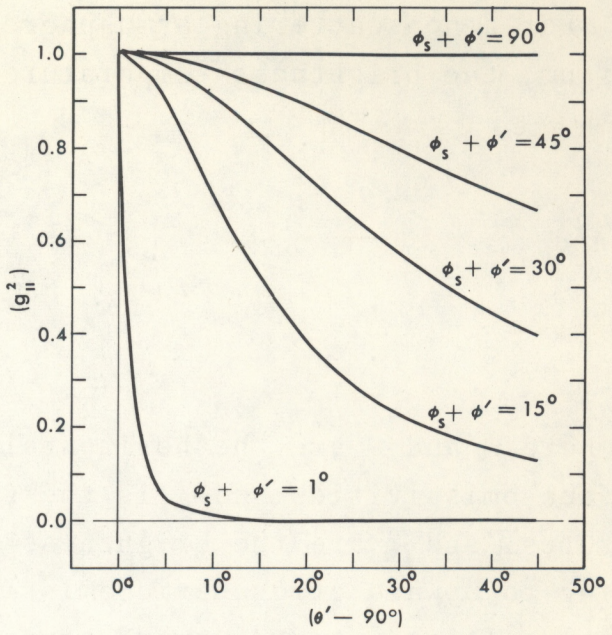


Figure 2.--Normalized horizontal emissivity component $(g_{11}^2)$ as a function of antenna angles $(\theta', \phi', \phi_s)$

Figure 2 shows a plot of $g_{11}^2$ as a function of zenith angle for a different azimuthal and scan angle. At nadir (here, $\phi'+\phi_s=0^\circ$ and $\theta'=90^\circ$), $g_{11}^2=1$ so that $\epsilon_s=\epsilon_h$; however, for a few degrees from the nadir direction, the vertical emissivity component becomes dominant. This anomalous behavior of the composite emissivity with angle arises from the transformation of the horizontal and vertical polarized radiation fields into antenna polarized field components. To further study this behavior, we compute the horizontal and vertical components of antenna temperature and determine their variations with scan angle and antenna beam width.

To obtain a measure of the energy received in horizontal and vertical polarization, we consider a clear atmosphere so that eq (11) becomes

$$\frac{T_a(\phi_s)}{T_s} = \frac{\iint G\epsilon_s \sin\theta' d\theta' d\phi'}{\iint G \sin\theta' d\theta' d\phi'} \qquad (13)$$

where use was made of the fact that $T_u = T_d = 0$ and $\tau = 1$ for a perfectly clear atmosphere. Equation (13) is analyzed for an antenna

viewing a flat surface from which the horizontal and vertical emissivities are considered constant within the antenna beam. Hence, using eq (11d), we reduce eq (13) to

$$\frac{T_a}{T_s} = \epsilon_h H + \epsilon_v V \tag{14a}$$

where

$$H = \frac{\iint G_h \sin\theta' d\theta' d\phi'}{\iint G \sin\theta' d\theta' d\phi'} \tag{14b}$$

and

$$H + V = 1. \tag{14c}$$

The terms $H$ and $V$ are measures of the relative amount of energy received in horizontal or vertical polarization, respectively. For illustrative purposes, an antenna is considered having the gain functions given by

$$G_{\theta'}(\theta', \phi') = \begin{cases} 1 & \frac{B}{2} \geq \phi' \geq -\frac{B}{2}, \quad 90° + \frac{B}{2} \geq \phi' \geq 90° - \frac{B}{2} \\ 0 & \text{all other angles} \end{cases} \tag{15a}$$

and

$$G_{\phi'}(\theta', \phi') = 0 \quad \text{for all angles.} \tag{15b}$$

Equation (15) defines the gain functions for a linearly polarized antenna with its polarization direction along $a_{\theta'}$. Effects due to cross polarization ($G_{\phi'} \neq 0$) will be discussed later.

Substituting eq (6), (8b), and (15) into eq (14b), we find that

$$H = \frac{\iint g_{11}^2 G_{\theta'} \sin\theta' d\theta' d\phi'}{\iint G_{\theta'} \sin\theta' d\theta' d\phi'} = \frac{2}{B} \int_0^{B/2} \frac{\tan^{-1}\left[\sin\frac{B}{2} \cdot \cot(\phi' + \phi_s)\right]}{\left[\sin\frac{B}{2} \cdot \cot(\phi' + \phi_s)\right]} d\phi' \tag{16}$$

where the angle $B$ is the antenna beam width.

Equation (16) is plotted in figure 3 as a function of scan angle $\phi_s$ for different beam widths $B$. Note that, for zero beam width $H=1$, $V=0$ so that all energy received is in horizontal polarization independent of scan angle. However, for increasing beam width, there are larger vertical polarization contributions for scan angles near nadir. This result indicates that a linearly polarized antenna scanned about its polarization axes receives predominantly horizontally polarized radiation; the influence of the vertically polarized radiation is significant only near nadir. At near-nadir directions, however, the horizontal and vertical emissivities are almost identical (see Stogryn 1972) so that the antenna temperature is essentially described by the horizontal component of emissivity for all scan angles.

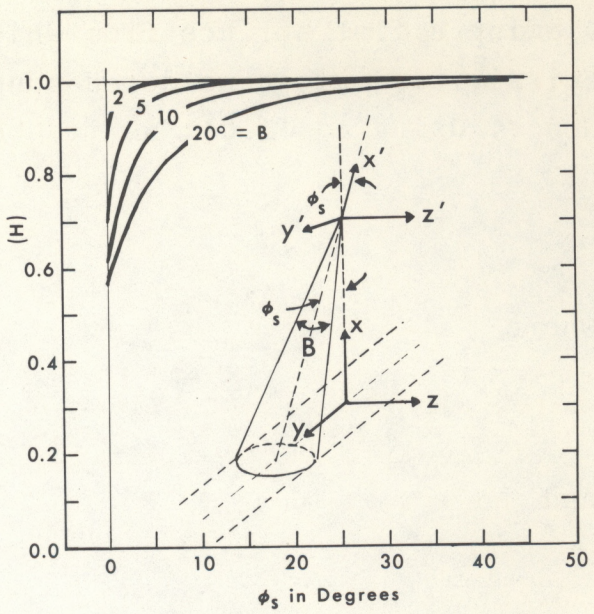


Figure 3.--Normalized power received in horizontal polarization ($H$) as a function of scan angle ($\phi_s$) for different beam widths ($B$)

## CROSS-POLARIZATION EFFECTS

The effects due to antenna cross-polarization are obtained using eq (14) and considering the primary polarization along $a_{\theta'}$ with gain $G_{\theta'}$ and cross polarization along $a_{\phi'}$ with gain $G_{\phi'}$. For simplicity, we consider the gain functions related by a constant parameter $\rho$, namely:

$$G_{\phi'} \equiv \frac{\rho}{1-\rho} G_{\theta'} \qquad 1 \geq \rho \geq 0 \tag{17}$$

where $\rho=0$ corresponds to a linearly polarized antenna with polarization $a_{\theta'}$ and $\rho=1$ refers to a linearly polarized antenna with orthogonal polarization $a_{\phi'}$ (considered cross-polarized direction).

Substituting eq (17) into eq (14), we obtain

$$H=\rho+(1-2\rho)H_0 \qquad (18a)$$

and

$$H_0=\frac{\iint g_{11}^2 G_{\theta'}\sin\theta'\,d\theta'\,d\phi'}{\iint G_{\theta'}\sin\theta'\,d\theta'\,d\phi'} \qquad (18b)$$

where $H_0$ is the result obtained for a linear polarized antenna with polarization $a_{\theta'}$.

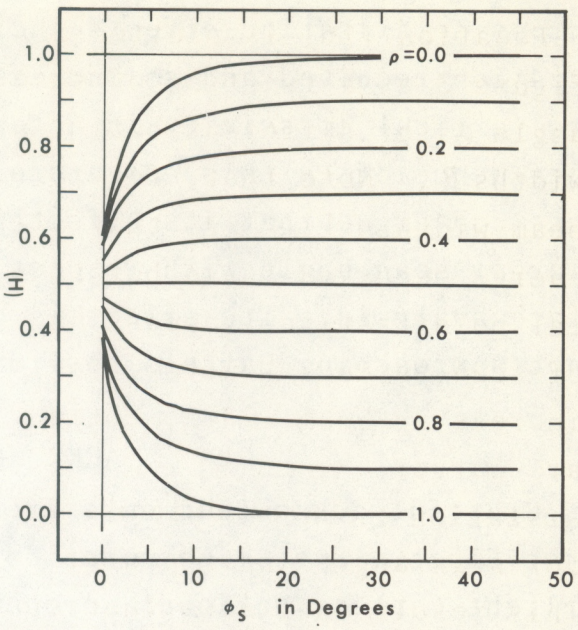


Figure 4.--Normalized power received in horizontal polarization ($H$) as a function of scan angle ($\phi_s$) for different amounts of cross polarization ($\rho$); antenna beam width ($B = 10°$)

After we use the gain function $G_{\theta'}$ of eq (15a), $H_0$ is given by eq (16). From figure 3, observe that $H_0$ is approximately unity for scan angles larger than the beam width. It then follows from eq (18a) that, for such scan angles, $H\cong 1-\rho$ and $V\cong\rho$, or the power received in vertical polarization is linearly related to the percent of cross polarization as given by the parameter $\rho$. Equation (18a) has the form shown in figure 4 for an antenna beam width of 10°. The effects due to cross polarization are to increase the level of power received in vertical polarization and alter the scan angle dependence of received radiation. It also appears that a minimization of the scan angle dependence can be achieved by receiving equal polarization in $a_{\theta'}$ and $a_{\phi'}$ (i.e., $\rho=1/2$).

## CONCLUSIONS

Analysis of a linearly polarized antenna scanned about its polarization axes leads to the interesting result that the power received is predominantly of horizontal polarization, except for near-nadir scan angles. Hence, the horizontal emissivity is to be used in such antenna temperature calculations. We found that

cross-polarization effects increase the level of vertical polarization received and so increase the contribution attributable to vertical emissivity in antenna temperature calculations. The influence of Earth's curvature has not been analyzed; however, one can argue that its effect is to give the appearance of a larger scan angle with respect to that employed in the flat surface analysis. Its effect is generally small for scan angles not approaching Earth's horizon.

## ACKNOWLEDGMENTS

Grateful acknowledgments are made to A. Stogryn of the Aerojet Electro-System Corporation and to J. Shue of Goddard Space Flight Center, National Aeronautics and Space Administration, for their suggestions and discussions during the preparation of this report.

## REFERENCES

Claassen, J.P., and Fung, A.R., "An Efficient Technique for Determining Apparent Temperature Distributions From Antenna Temperature Measurements," Technical Report 186-8, University of Kansas Center for Research, Lawrence, Kans., Sept. 1973, 33 pp.

Stogryn, A., "The Brightness Temperature of a Vertically Structured Medium," Radio Science, Vol. 5, No. 12, Dec. 1970, p. 1400.

Stogryn, A., "A Study of Radiometric Emission From a Rough Sea Surface," Technical Report 300R-1, Aerojet Electro-System Corporation, Azusa, Calif., July 1972, pp. 40-42.

## APPENDIX: DERIVATION OF THE GEOMETRIC MATRIX ELEMENTS

$$\mathcal{G}_{11} = \mathbf{a}_{\theta'} \cdot \frac{\mathbf{n} \times \mathbf{k}'}{|\mathbf{n} \times \mathbf{k}'|} = -\frac{(\mathbf{a}_{\theta'} \times \mathbf{k}') \cdot \mathbf{n}}{|\mathbf{n} \times \mathbf{k}'|}, \tag{19}$$

$$\mathcal{G}_{12} = \mathbf{a}_{\theta'} \cdot \frac{(\mathbf{n} \times \mathbf{k}') \times \mathbf{k}'}{|(\mathbf{n} \times \mathbf{k}') \times \mathbf{k}'|} = -\frac{\mathbf{a}_{\theta'} \cdot \mathbf{n}}{|(\mathbf{n} \times \mathbf{k}') \times \mathbf{k}'|} \quad \text{since } \mathbf{a}_{\theta'} \cdot \mathbf{k}' = 0, \tag{20}$$

$$\mathcal{G}_{21} = \mathbf{a}_{\phi'} \cdot \frac{\mathbf{n} \times \mathbf{k}'}{|\mathbf{n} \times \mathbf{k}'|} = -\frac{(\mathbf{a}_{\phi'} \times \mathbf{k}') \cdot \mathbf{n}}{|\mathbf{n} \times \mathbf{k}'|}, \tag{21}$$

and

$$\mathcal{G}_{22} = \mathbf{a}_{\phi'} \cdot \frac{(\mathbf{n} \times \boldsymbol{\kappa}') \times \boldsymbol{\kappa}'}{|(\mathbf{n} \times \boldsymbol{\kappa}') \times \boldsymbol{\kappa}'|} = - \frac{\mathbf{a}_{\phi'} \cdot \mathbf{n}}{|(\mathbf{n} \times \boldsymbol{\kappa}') \times \boldsymbol{\kappa}'|} \quad \text{since } \mathbf{a}_{\phi'} \cdot \boldsymbol{\kappa}' = 0. \tag{22}$$

Also,

$$|\mathbf{n} \times \boldsymbol{\kappa}'| = \sqrt{(\mathbf{n} \times \boldsymbol{\kappa}') \cdot (\mathbf{n} \times \boldsymbol{\kappa}')} = \sqrt{(\mathbf{n} \times \boldsymbol{\kappa}') \times \mathbf{n} \cdot \boldsymbol{\kappa}'}$$

$$= \sqrt{[\boldsymbol{\kappa}' - \mathbf{n}\,(\boldsymbol{\kappa}' \cdot \mathbf{n})] \cdot \boldsymbol{\kappa}'} = \sqrt{1 - (\boldsymbol{\kappa}' \cdot \mathbf{n})^2}\,, \tag{23}$$

and

$$|(\mathbf{n} \times \boldsymbol{\kappa}') \times \boldsymbol{\kappa}'| = \sqrt{(\mathbf{n} \times \boldsymbol{\kappa}') \times \boldsymbol{\kappa}' \cdot (\mathbf{n} \times \boldsymbol{\kappa}') \times \boldsymbol{\kappa}'} = \sqrt{[\boldsymbol{\kappa}' - \mathbf{n}(\boldsymbol{\kappa}' \cdot \mathbf{n})] \cdot [\boldsymbol{\kappa}' - \mathbf{n}(\boldsymbol{\kappa}' \cdot \mathbf{n})]}$$

$$= \sqrt{(\boldsymbol{\kappa} \cdot \mathbf{n})^2 + 1 - 2\,(\boldsymbol{\kappa} \cdot \mathbf{n})^2} = \sqrt{1 - (\boldsymbol{\kappa}' \cdot \mathbf{n})^2}\,. \tag{24}$$

Using the relationships,

$$\mathbf{a}_{\theta'} \times \boldsymbol{\kappa}' = - \mathbf{a}_{\phi'} \quad \text{and} \quad \mathbf{a}_{\phi'} \times \boldsymbol{\kappa}' = \mathbf{a}_{\theta'},$$

$$\mathcal{G}_{11} = - \mathcal{G}_{22} = \frac{\mathbf{a}_{\phi'} \cdot \mathbf{n}}{\sqrt{1 - (\boldsymbol{\kappa}' \cdot \mathbf{n})^2}} \tag{25}$$

and

$$\mathcal{G}_{12} = \mathcal{G}_{21} = - \frac{\mathbf{a}_{\phi'} \cdot \mathbf{n}}{\sqrt{1 - (\boldsymbol{\kappa}' \cdot \mathbf{n})^2}}\,. \tag{26}$$

Now,

$$\mathbf{E} \cdot \mathbf{E} = E_h^2 + E_v^2 = E_{\theta'}^2 + E_{\phi'}^2$$

so that, substituting eq (2) into this equation and using eq (7a) and (8a), we obtain

$$\mathcal{G}_{11}^2 + \mathcal{G}_{12}^2 = 1$$

or

$$\mathcal{G}_{12} = \sqrt{1 - \mathcal{G}_{11}^2}\,. \tag{27}$$

☆ U.S. GOVERNMENT PRINTING OFFICE : 1974—542-653/135

(Continued from inside front cover)

NESC 51 Application of Meteorological Satellite Data in Analysis and Forecasting. Ralph K. Anderson, Jerome P. Ashman, Fred Bittner, Golden R. Farr, Edward W. Ferguson, Vincent J. Oliver, and Arthur H. Smith, September 1969. Price $1.75 (AD-697-033) Supplement price $0.65 (AD-740-017)

NESC 52 Data Reduction Processes for Spinning Flat-Plate Satellite-Borne Radiometers. Torrence H. MacDonald, July 1970. Price $0.50 (COM-71-00132)

NESC 53 Archiving and Climatological Applications of Meteorological Satellite Data. John A. Leese, Arthur L. Booth, and Frederick A. Godshall, July 1970. Price $1.25 (COM-71-00076)

NESC 54 Estimating Cloud Amount and Height From Satellite Infrared Radiation Data. P. Krishna Rao, July 1970. Price $0.25 (PB-194-685)

NESC 56 Time-Longitude Sections of Tropical Cloudiness (December 1966-November 1967). J. M. Wallace, July 1970. Price $0.50 (COM-71-00131)

NOAA Technical Reports

NESS 55 The Use of Satellite-Observed Cloud Patterns in Northern Hemisphere 500-mb Numerical Analysis. Roland E. Nagle and Christopher M. Hayden, April 1971. Price $0.55 (COM-73-50262)

NESS 57 Table of Scattering Function of Infrared Radiation for Water Clouds. Giichi Yamamoto, Masayuki Tanaka, and Shoji Asano, April 1971. Price $1.00 (COM-71-50312)

NESS 58 The Airborne ITPR Brassboard Experiment. W. L. Smith, D. T. Hilleary, E. C. Baldwin, W. Jacob, H. Jacobowitz, G. Nelson, S. Soules, and D. Q. Wark, March 1972. Price $1.25 (COM-72-10557)

NESS 59 Temperature Sounding From Satellites. S. Fritz, D. Q. Wark, H. E. Fleming, W. L. Smith, H. Jacobowitz, D. T. Hilleary, and J. C. Alishouse, July 1972. Price $0.55 (COM-72-50963)

NESS 60 Satellite Measurements of Aerosol Backscattered Radiation From the Nimbus F Earth Radiation Experiment. H. Jacobowitz, W. L. Smith, and A. J. Drummond, August 1972. Price $0.25 (COM-72-51031)

NESS 61 The Measurement of Atmospheric Transmittance From Sun and Sky With an Infrared Vertical Sounder. W. L. Smith and H. B. Howell, September 1972. Price $0.30 (COM-73-50020)

NESS 62 Proposed Calibration Target for the Visible Channel of a Satellite Radiometer. K. L. Coulson and H. Jacobowitz, October 1972. Price $0.35 (COM-73-10143)

NESS 63 Verification of Operational SIRS B Temperature Retrievals. Harold J. Brodrick and Christopher M. Hayden, December 1972. Price $0.55 (COM-73-50279)

NESS 64 Radiometric Techniques for Observing the Atmosphere From Aircraft. William L. Smith and Warren J. Jacob. January 1973. Price $0.35 (COM-73-50376)

NESS 65 Satellite Infrared Soundings From NOAA Spacecraft. L. M. McMillin, D. Q. Wark, J.M. Siomkajlo, P. G. Abel, A. Werbowetzki, L. A. Lauritson, J. A. Pritchard, D. S. Crosby, H. M. Woolf, R. C. Luebbe, M. P. Weinreb, H. E. Fleming, F. E. Bittner, and C. M. Hayden, September 1973. Price $1.30 (COM-73-50936/6AS)

NESS 66 Effects of Aerosols on the Determination of the Temperature of the Earth's Surface From Radiance Measurements at 11.2 μm. H. Jacobowitz and K. L. Coulson, September 1973. Price $0.55 (COM-74-50013)

NESS 67 Vertical Resolution of Temperature Profiles for High Resolution Infrared Radiation Sounder (HIRS). Y. M. Chen, H. M. Woolf, and W. L. Smith, January 1974.